Prethermalization and Thermalization in Models with Weak Integrability Breaking

Bruno Bertini,[1] Fabian H. L. Essler,[1] Stefan Groha,[1] and Neil J. Robinson[1,2]
[1]The Rudolf Peierls Centre for Theoretical Physics, University of Oxford, Oxford, OX1 3NP, United Kingdom
[2]Condensed Matter Physics and Materials Science Department, Brookhaven National Laboratory, Upton, New York 11973, USA
(Received 15 June 2015; published 29 October 2015)

We study the effects of integrability-breaking perturbations on the nonequilibrium evolution of many-particle quantum systems. We focus on a class of spinless fermion models with weak interactions. We employ equation of motion techniques that can be viewed as generalizations of quantum Boltzmann equations. We benchmark our method against time-dependent density matrix renormalization group computations and find it to be very accurate as long as interactions are weak. For small integrability breaking, we observe robust prethermalization plateaux for local observables on all accessible time scales. Increasing the strength of the integrability-breaking term induces a "drift" away from the prethermalization plateaux towards thermal behavior. We identify a time scale characterizing this crossover.

DOI: 10.1103/PhysRevLett.115.180601 PACS numbers: 05.70.Ln, 03.75.Ss, 71.10.Fd, 71.10.Pm

In classical mechanics, integrable few-particle systems can be understood in terms of periodic, nonergodic motion in action-angle variables. Breaking integrability by adding a weak perturbation induces a fascinating crossover between integrable and chaotic motion, which is described by the celebrated Kolmogorov-Arnold-Moser theory [1]. In essence, classical few-particle systems with weak integrability breaking retain aspects of integrable motion on intermediate time scales. Recently, it has emerged that similar behavior occurs in the nonequilibrium evolution of isolated many-particle quantum systems. Starting with the seminal work of Rigol *et al.* [2], it has become clear that there is a dramatic difference between the late time behavior of isolated integrable and nonintegrable quantum many-particle systems prepared in initial states that are not eigenstates of the Hamiltonian. Generic systems *thermalize* [2–13], i.e., exhibit relaxation of local observables towards a Gibbs ensemble with an effective temperature, while integrable systems evolve towards a generalized Gibbs ensemble [2,12–35]. Starting with the work of Moeckel and Kehrein [36], it was then realized that models with weak integrability-breaking perturbations exhibit transient behavior, in which local observables relax towards nonthermal values that retain information of the proximate integrable theory. This has been termed *prethermalization* and has been established to occur in several models [36–46]. Crucially, it was recently observed in experiments on ultracold bosonic atoms [47–49]. The general expectation is that prethermalization is a transient effect, and at "sufficiently late times" nonintegrable systems thermalize. While this appears natural, there is scant evidence in support of this scenario. The reason is that available numerical [50] or analytical [36,41,45] methods are not able to reach late enough times. The exception is the case of infinitely many dimensions, where it was shown in a particular example that a weakly nonintegrable model thermalizes [51]. Here we address these issues in the context of weakly interacting one-dimensional many-particle systems. This case has the important advantage that the accuracy of approximate methods can be benchmarked by comparisons with powerful numerical methods like the time-dependent density matrix renormalization group (t-DMRG) [50]. Moreover, the existence of many strongly interacting one-dimensional integrable systems makes it possible to verify that the qualitative behavior we find persists for arbitrary interaction strengths.

We focus on the weak interaction regime $U \lesssim J_1$ of the three-parameter family of spinless fermion Hamiltonians

$$H(J_2,\delta,U) = -J_1 \sum_{l=1}^{L} [1+(-1)^l\delta](c_l^\dagger c_{l+1} + \text{H.c.}) - J_2 \sum_{l=1}^{L} [c_l^\dagger c_{l+2} + \text{H.c.}] + U \sum_{l=1}^{L} n_l n_{l+1}. \quad (1)$$

Here c_i and $c_i^\dagger$ are spinless fermion operators on site i, and the hopping amplitudes describe nearest-neighbor and next-nearest-neighbor hopping, respectively, while $0 \le \delta < 1$ is a dimerization parameter. Finally, there is a repulsive nearest-neighbor interaction of strength U. From here onwards, we set $J_1 = 1$ and measure all the energies in units of J_1. There are a several limits in which (1) becomes integrable: (i) $U = 0$ describes a free theory; (ii) $\delta = J_2 = 0$ corresponds to the anisotropic spin-1/2 Heisenberg chain [52]; (iii) the low-energy degrees of freedom for $J_2 = 0$ and $\delta\, U \ll 1$ are described by the quantum sine-Gordon model [53]. Away from these limits, the model is nonintegrable. Our protocol for inducing and analyzing nonequilibrium dynamics is as follows. We prepare the system in an initial density matrix ρ_0 that is not an eigenstate of $H(J_2,\delta,U)$ for any value of U. We then compare the expectation values of local operators for time evolution with the integrable

$H(J_2,\delta,0)$ and (weakly) nonintegrable $H(J_2,\delta,U)$, respectively. For $U=0$ our model is noninteracting, and concomitantly in the thermodynamic limit expectation values of local operators relax to time-independent values described by a generalized Gibbs ensemble. In the following, we analyze how a small integrability-breaking interaction $U>0$ changes the nonequilibrium evolution. We stress that our protocol differs in a very important way from the weak interaction quenches analyzed previously [51,54]. In these works, there is no dynamics at all for $U=0$. Hence, quenching the interaction from zero to a finite value simultaneously breaks integrability and induces a time dependence into the problem. This masks the interaction-induced modification of the integrable postquench dynamics. Quantum quenches in the model (1) with $J_2=0$ were previously studied in Ref. [41] by numerical and analytical methods. On the accessible time scales, robust prethermalization was observed, but no evidence for eventual thermalization was found. Recently, a paper appeared in which techniques similar to the ones we employ here were used to analyze quantum quenches in the case $\delta_i=\delta_f=0$ [54]. No prethermalization in our sense was observed for the aforementioned reason that there is no dynamics without integrability breaking in this case, but instead evolution towards a thermal steady state was found. Given that U is small, a convenient basis for analyzing quench dynamics is obtained by diagonalizing the quadratic part of the Hamiltonian. This results in

$$H(J_2,\delta,0)=\sum_{\alpha=\pm}\sum_{k>0}\epsilon_\alpha(k)a_\alpha^\dagger(k)a_\alpha(k), \tag{2}$$

where $a_\pm(k)$ are momentum space annihilation operators obeying canonical anticommutation relations $\{a_\alpha(k),a_\beta^\dagger(q)\}=\delta_{\alpha,\beta}\delta_{k,q}$ and $\epsilon_\alpha(k)=-2J_2\cos(2k)+2\alpha\sqrt{\delta^2+(1-\delta^2)\cos^2(k)}$ are single-particle dispersion relations of the two bands of fermions. The system is initially (at time $t=0$) prepared in a density matrix ρ_0 and subsequently evolves according to

$$\rho(t)=e^{-iH(J_2,\delta_f,U)t}\rho_0 e^{iH(J_2,\delta_f,U)t}. \tag{3}$$

Using equation of motion (EOM) techniques [51,55] analogous to the ones employed in derivations of quantum Boltzmann equations [56,57], we obtain evolution equations for the two-point functions:

$$n_{\alpha\beta}(q,t)=\mathrm{Tr}[\rho(t)a_\alpha^\dagger(q)a_\beta(q)]. \tag{4}$$

The EOM can be cast in the form

$$\begin{aligned}\dot n_{\alpha\beta}(k,t)=&\,i\epsilon_{\alpha\beta}(k)n_{\alpha\beta}(k,t)+4iUe^{it\epsilon_{\alpha\beta}(k)}\sum_{\gamma_1}J_{\gamma_1\alpha}(k;t)n_{\gamma_1\beta}(k,0)-J_{\beta\gamma_1}(k;t)n_{\alpha\gamma_1}(k,0)\\&-U^2\int_0^t dt'\sum_\gamma\sum_{k_1,k_2>0}K^\gamma_{\alpha\beta}(k_1,k_2;k;t-t')n_{\gamma_1\gamma_2}(k_1,t')n_{\gamma_3\gamma_4}(k_2,t')\\&-U^2\int_0^t dt'\sum_{\underline\gamma}\sum_{k_1,k_2,k_3>0}L^{\underline\gamma}_{\alpha\beta}(k_1,k_2,k_3;k;t-t')n_{\gamma_1\gamma_2}(k_1,t')n_{\gamma_3\gamma_4}(k_2,t')n_{\gamma_5\gamma_6}(k_3,t'),\end{aligned} \tag{5}$$

where $\epsilon_{\alpha\beta}(k)=\epsilon_\alpha(k)-\epsilon_\beta(k)$. Explicit expressions for the kernels J, K, and L and details of our derivation are given in Supplemental Material [58]. The solution of the set of integro-differential equations (5) is numerically demanding. We designed an algorithm that scales as $L^3\times T$, where T is the number of time steps and L the number of lattice sites. This allows us to reach long times $J_1t\sim 80$ on large systems $L\sim 320$ (a similar scaling was proposed in Ref. [54]). Given the expectation values (4), we may readily calculate the single-particle Green's function

$$\begin{aligned}\mathcal{G}(j,l;t)&=\mathrm{Tr}[\rho(t)c_j^\dagger c_l]\\&=\frac{1}{L}\sum_{k>0}\sum_{\alpha,\beta=\pm}\gamma_\alpha^*(k,j)\gamma_\beta(k,l)n_{\alpha\beta}(k,t),\end{aligned} \tag{6}$$

where the coefficients $\gamma_\alpha(k,j)$ are given in Supplemental Material [58]. A crucial check of the accuracy of our approach is provided by a direct comparison to previous t-DMRG computations [41]. In Fig. 1, we present a comparison of $\mathcal{G}(L/2,L/2+1)$ between EOM and t-DMRG results for a quench where the system is prepared in the ground state of $H(0,0.8,0)$ and time evolved subject to the Hamiltonian $H(0,0.4,0.4)$. We see that, even for relatively large $U=0.4$, there is excellent agreement between the two methods for all times accessible by t-DMRG. Similar levels of agreement are found for other $\mathcal{G}(L/2,L/2+j)$ with $j=2,3,4,5$. This agreement suggests that the EOM method is very accurate for small values of U and short and intermediate time scales. The advantage of the EOM method is that it allows us to access later time scales than the t-DMRG computations reported in Ref. [41]. As long as the interaction strength U is sufficiently small, we observe very long-lived prethermalization plateaux, as is exemplified in the inset in Fig. 1.

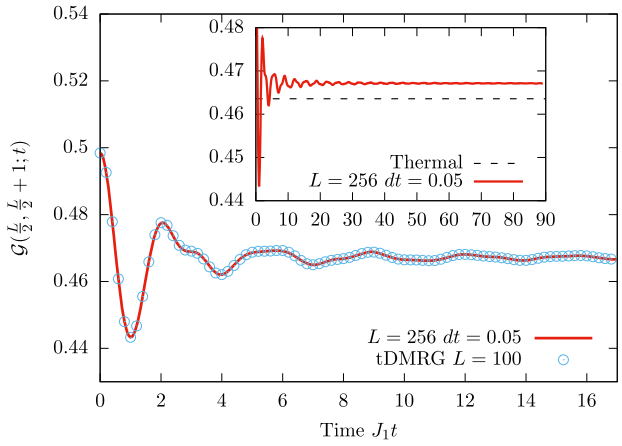

FIG. 1 (color online). $\mathcal{G}(L/2, L/2+1; t)$ for a quench where the system is prepared in the ground state of $H(0, 0.8, 0)$ and time evolved with $H(0, 0.4, 0.4)$ for a system with $L = 256$ sites. The EOM results (red line) are in excellent agreement with t-DMRG computations [41] (circles). Inset: Prethermalized behavior persists over a large time interval.

There, the thermal value has been computed by quantum Monte Carlo simulations on a system with $L = 100$ sites.

In order to investigate if and how the prethermalized regime evolves towards thermal equilibrium, it is convenient to invoke a nonzero J_2. In essence, J_2 allows us to tune the crossover time scale between the two regimes. In order to access the dynamics for a larger range of energy densities, we consider thermal initial density matrices of the form

$$\rho(\beta, J_2, \delta, U) = \frac{e^{-\beta H(J_2,\delta,U)}}{\mathrm{Tr}(e^{-\beta H(J_2,\delta,U)})}. \quad (7)$$

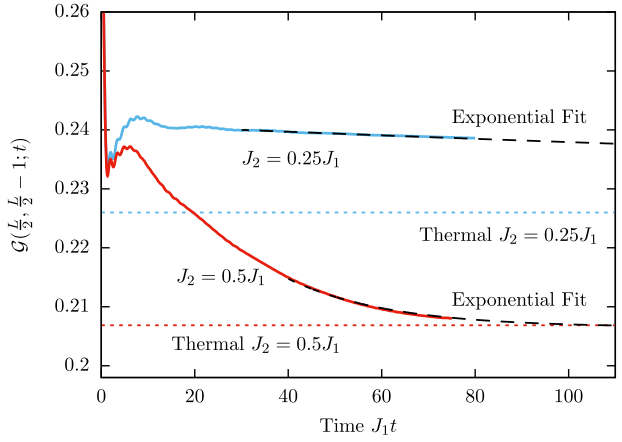

FIG. 2 (color online). $\mathcal{G}(L/2, L/2-1; t)$ for a system with Hamiltonian $H(J_2, 0.1, 0.4)$ and sizes $L = 360, 320$ initially prepared in a thermal state (7) with density matrix $\rho(2, 0, 0, 0)$. The expected steady state thermal values are indicated by dotted lines, while the black dashed lines are exponential fits to (8).

Figures 2 and 3 show results for the time evolution of the Green's function for a system prepared in the initial state (7) with density matrix $\rho(2, 0, 0, 0)$ and time evolved with Hamiltonian $H(J_2, 0.1, 0.4)$. In contrast to the case $J_2 = 0$, $U = 0.4$, we now observe a slow drift towards a thermal steady state. Increasing J_2 enhances the drift. The thermal values shown in Figs. 2 and 3 are obtained as follows. The energy density is given by $e = \mathrm{Tr}[\rho(2, 0, 0, 0) H(J_2, 0.1, 0.4)]/L$ and determines the effective temperature $1/\beta_{\mathrm{eff}}$ of the thermal ensemble for the postquench Hamiltonian $H(J_2, 0.1, 0.4)$ through $e = \mathrm{Tr}[\rho(\beta_{\mathrm{eff}}, J_2, 0.1, 0.4) H(J_2, 0.1, 0.4)]/L$ [59]. We determine β_{eff} by exact diagonalization of small systems up to size $L = 16$ and then use the same method to compute the single-particle Green's function in thermal equilibrium at temperature $1/\beta_{\mathrm{eff}}$. We note that $\mathcal{G}(i, j; t)$ is real for odd separations $|i - j|$. For even $|i - j|$, the imaginary part is nonzero but small and relaxes towards zero. We find that the observed relaxation towards thermal values is compatible with exponential decay

$$\mathcal{G}(i, j; t) \sim \mathcal{G}(i, j)_{\mathrm{th}} + A_{ij}(J_2, \delta, U) e^{-t/\tau_{ij}(J_2,\delta,U)}, \quad (8)$$

where $\mathcal{G}(i, j)_{\mathrm{th}}$ is the thermal Green's function at temperature $1/\beta_{\mathrm{eff}}$ [60]. The decay times $\tau_{ij}(J_2, \delta, U)$ are quite sensitive to the value of J_2. This can be understood by noting that large values of J_2 modify the band structure of the noninteracting model by introducing additional crossings at a fixed energy. This, in turn, generates additional scattering channels that promote relaxation.

A natural question is whether the integral equation (5) can be simplified in the late time regime by removing the time integration, in analogy with standard quantum Boltzmann equations (QBE) [56,57]. Here we are faced

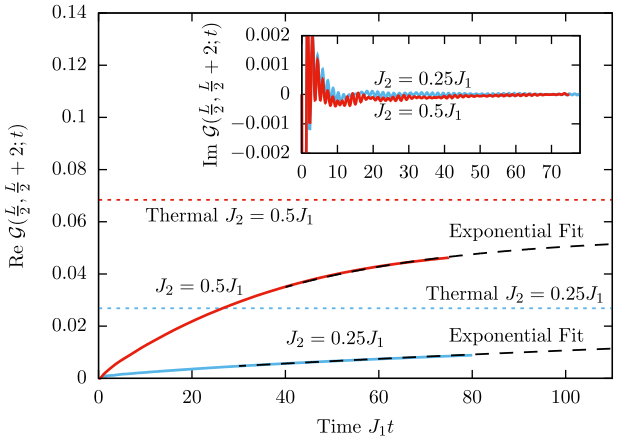

FIG. 3 (color online). Real (inset, imaginary) part of $\mathcal{G}(L/2, L/2+2; t)$ for a system with Hamiltonian $H(J_2, 0.1, 0.4)$ and sizes $L = 360, 320$, that was initially prepared in a thermal state (7) with density matrix $\rho(2, 0, 0, 0)$. The expected steady state thermal values are indicated by dotted lines, while the black dashed lines are exponential fits to (8).

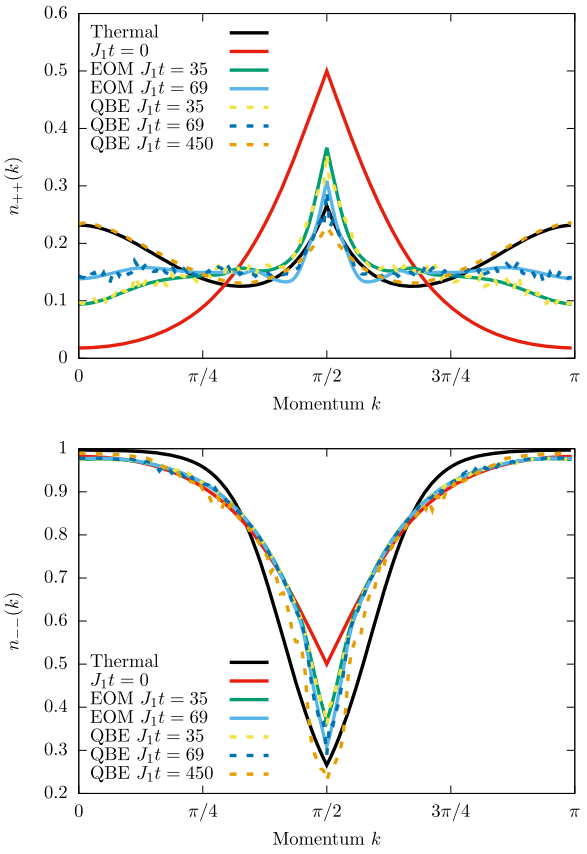

FIG. 4 (color online). Occupation numbers $n_{++}(k,t)$ and $n_{--}(k,t)$ initialized in the thermal state (7) $\rho(2,0,0.5,0)$ and time evolved with $H(0.5,0,0.4)$. The solid lines are the results of the EOM ($L = 320$) for various times. The dotted lines are computed by means of the QBE ($L = 320$). The black solid line is the thermal value found by means of second-order perturbation theory in U.

with the difficulty that the structure of our EOM (5) is quite different from the ones studied in Refs. [56,57]. However, in the case $\delta_f = 0$, numerical integration of the full EOM (5) suggests that the "off-diagonal" occupation numbers become negligible at late times $n_{+-}(k,t) \approx 0$ and it is possible to derive a QBE for "diagonal" occupation numbers. The QBE for $\delta_f = 0$ reads

$$\dot{n}_{\alpha\alpha}(k,\tau) = -\sum_{\gamma,\delta}\sum_{p,q>0} \tilde{K}^{\gamma\delta}_{\alpha\alpha}(p,q;k) n_{\gamma\gamma}(p,\tau) n_{\delta\delta}(q,\tau) - \sum_{\gamma,\delta,\epsilon}\sum_{p,q,r>0} \tilde{L}^{\gamma\delta\epsilon}_{\alpha\alpha}(p,q,r;k) n_{\gamma\gamma}(p,\tau) \times n_{\delta\delta}(q,\tau) n_{\epsilon\epsilon}(r,\tau). \quad (9)$$

Here $\tau = U^2 t$ is the usual rescaled time variable, $t_0 \gg 1/U$ is the time at which the kinetic equation is initialized, and the functions $\tilde{K}, \tilde{L}$ are given in Supplemental Material [58]. The QBE agrees with the EOM for sufficiently late times (an example is shown in Fig. 4; see the discussion below).

Because of its simpler structure, the QBE allows us to access later times than we are able to reach with the EOM approach. In particular, employing the QBE we conclude that for weak interactions the relaxation times in (8) scale as [61]

$$\tau_{ij}^{-1}(J_2, \delta_f = 0, U) \propto U^2. \quad (10)$$

This is in contrast to the U^4 scaling found for interaction quenches in the infinite-dimensional Hubbard model [51].

To establish more comprehensively that the integrability-breaking perturbation leads to thermalization, we consider the (Bogoliubov) mode occupation numbers $n_{\alpha\beta}(q,t)$ themselves. The mode occupation operators are not local in space, and hence it is not *a priori* clear that their expectation values should eventually thermalize; see, however, Ref. [62]. Importantly, we consider only initial states with finite correlation lengths, which implies that $\mathcal{G}(j,l;t)$ are exponentially small in $|j-l|$ as long as $|j-l| \gg J_1 t$ [63]. This, together with the fact that $\mathcal{G}(j,l;t)$ decay exponentially fast in time for $|j-l| \leq J_1 t$, suggests that $n_{\alpha\beta}(q,t)$ should relax in the regime $1 \ll J_1 t \ll L$. In Fig. 4, we present the mode occupation numbers $n_{\alpha\alpha}(k,t)$ at several different times for a system of size $L = 320$ prepared in the density matrix $\rho(2,0,0.5,0)$ and evolved with Hamiltonian $H(0.5,0,0.4)$. For short and intermediate times $J_1 t < 70$, we use the full EOM, while late times are accessible only to the QBE. The QBE is initialized at time $t_0 = 20$ and is seen to be in good agreement with the full EOM until the latest times accessible by the latter method. We observe that at intermediate times both $n_{++}(k,t)$ and $n_{--}(k,t)$ slowly approach their respective thermal distributions at the effective temperature $1/\beta_{\text{eff}}$ introduced above. The off-diagonal occupation numbers $n_{+-}(k,t)$, calculated by integrating the full EOM, approach their thermal value zero in an oscillatory fashion. The observed behavior of the mode occupation numbers strongly suggests that the weak integrability-breaking term indeed induces thermalization.

We note that in the QBE framework the final relaxation is towards the noninteracting Fermi-Dirac distribution with an effective temperature set by the kinetic energy at the time the Boltzmann is initialized [57,64], signaling the importance of corrections to the QBE at very late times. Such corrections, arising from higher cumulants, are important for obtaining the power law behavior expected at very late times (for certain observables) after quenches in nonintegrable models [65,66].

In this work, we have developed a method that allows us to analyze the effects of a weak integrability-breaking interaction on the time evolution of local observables after a quantum quench. We have shown that there is a crossover between a prethermalized regime, characterized by the proximity of our model to an integrable theory, and a thermal steady state. The observed drift of $\mathcal{G}(i,j;t)$ in time

towards its thermal value is exponential and characterized by a time scale proportional to U^{-2}. The models considered here feature a global $U(1)$ symmetry (particle number conservation). A preliminary analysis suggests that the scenario found here, a prethermalized regime followed by a crossover to a thermal steady state, occurs also in the absence of this $U(1)$ symmetry [61].

We thank M. Fagotti, A. Gambassi, S. Kehrein, and A. Silva for helpful discussions. This work was supported by the EPSRC under Grants No. EP/J014885/1 and No. EP/I032487/1, by the U.S. Department of Energy, Office of Basic Energy Sciences, under Contracts No. DEAC02-98CH10886 and No. DE-SC0012704 (N. J. R.) and by the Clarendon Scholarship fund (S. G.).

[1] V. I. Arnold, *Mathematical Methods of Classical Mechanics* (Springer, New York, 1989).
[2] M. Rigol, V. Dunjko, V. Yurovsky, and M. Olshanii, Phys. Rev. Lett. **98**, 050405 (2007).
[3] J. M. Deutsch, Phys. Rev. A **43**, 2046 (1991).
[4] M. Srednicki, Phys. Rev. E **50**, 888 (1994).
[5] M. Rigol, V. Dunjko, and M. Olshanii, Nature (London) **452**, 854 (2008).
[6] M. Rigol, Phys. Rev. Lett. **103**, 100403 (2009).
[7] M. Rigol and L. F. Santos, Phys. Rev. A **82**, 011604(R) (2010).
[8] G. Biroli, C. Kollath, and A. M. Läuchli, Phys. Rev. Lett. **105**, 250401 (2010).
[9] M. C. Bañuls, J. I. Cirac, and M. B. Hastings, Phys. Rev. Lett. **106**, 050405 (2011).
[10] M. Tavora and A. Mitra, Phys. Rev. B **88**, 115144 (2013).
[11] M. Rigol, Phys. Rev. Lett. **112**, 170601 (2014).
[12] A. Polkovnikov, K. Sengupta, A. Silva, and M. Vengalattore, Rev. Mod. Phys. **83**, 863 (2011).
[13] C. Gogolin and J. Eisert, arXiv:1503.07538.
[14] M. Rigol, A. Muramatsu, and M. Olshanii, Phys. Rev. A **74**, 053616 (2006).
[15] M. A. Cazalilla, Phys. Rev. Lett. **97**, 156403 (2006).
[16] P. Calabrese and J. Cardy, J. Stat. Mech. (2007) P06008.
[17] M. Cramer, C. M. Dawson, J. Eisert, and T. J. Osborne, Phys. Rev. Lett. **100**, 030602 (2008).
[18] T. Barthel and U. Schollwöck, Phys. Rev. Lett. **100**, 100601 (2008).
[19] D. Fioretto and G. Mussardo, New J. Phys. **12**, 055015 (2010).
[20] P. Calabrese, F. H. L. Essler, and M. Fagotti, Phys. Rev. Lett. **106**, 227203 (2011); J. Stat. Mech. (2012) P07022.
[21] M. Fagotti and F. H. L. Essler, Phys. Rev. B **87**, 245107 (2013).
[22] J.-S. Caux and R. M. Konik, Phys. Rev. Lett. **109**, 175301 (2012).
[23] F. H. L. Essler, S. Evangelisti, and M. Fagotti, Phys. Rev. Lett. **109**, 247206 (2012).
[24] M. Collura, S. Sotiriadis, and P. Calabrese, Phys. Rev. Lett. **110**, 245301 (2013).
[25] G. Mussardo, Phys. Rev. Lett. **111**, 100401 (2013).
[26] B. Pozsgay, J. Stat. Mech. (2013) P07003.
[27] M. Fagotti and F. H. L. Essler, J. Stat. Mech. (2013) P07012.
[28] M. Fagotti, M. Collura, F. H. L. Essler, and P. Calabrese, Phys. Rev. B **89**, 125101 (2014).
[29] B. Wouters, J. De Nardis, M. Brockmann, D. Fioretto, M. Rigol, and J.-S. Caux, Phys. Rev. Lett. **113**, 117202 (2014).
[30] B. Pozsgay, M. Mestyán, M. A. Werner, M. Kormos, G. Zaránd, and G. Takács, Phys. Rev. Lett. **113**, 117203 (2014).
[31] M. Kormos, M. Collura, and P. Calabrese, Phys. Rev. A **89**, 013609 (2014).
[32] J. De Nardis, B. Wouters, M. Brockmann, and J.-S. Caux, Phys. Rev. A **89**, 033601 (2014).
[33] S. Sotiriadis and P. Calabrese, J. Stat. Mech. (2014) P07024.
[34] G. Goldstein and N. Andrei, Phys. Rev. A **90**, 043625 (2014).
[35] F. H. L. Essler, G. Mussardo, and M. Panfil, Phys. Rev. A **91**, 051602(R) (2015).
[36] M. Moeckel and S. Kehrein, Phys. Rev. Lett. **100**, 175702 (2008); Ann. Phys. (Amsterdam) **324**, 2146 (2009).
[37] A. Rosch, D. Rasch, B. Binz, and M. Vojta, Phys. Rev. Lett. **101**, 265301 (2008).
[38] M. Kollar, F. A. Wolf, and M. Eckstein, Phys. Rev. B **84**, 054304 (2011).
[39] M. van den Worm, B. C. Sawyer, J. J. Bollinger, and M. Kastner, New J. Phys. **15**, 083007 (2013).
[40] M. Marcuzzi, J. Marino, A. Gambassi, and A. Silva, Phys. Rev. Lett. **111**, 197203 (2013).
[41] F. H. L. Essler, S. Kehrein, S. R. Manmana, and N. J. Robinson, Phys. Rev. B **89**, 165104 (2014).
[42] N. Nessi, A. Iucci, and M. A. Cazalilla, Phys. Rev. Lett. **113**, 210402 (2014).
[43] M. Fagotti, J. Stat. Mech. (2014) P03016.
[44] G. P. Brandino, J.-S. Caux, and R. M. Konik, arXiv:1407.7167 [Phys. Rev. X (to be published)].
[45] B. Bertini and M. Fagotti, J. Stat. Mech. (2015) P07012.
[46] M. Babadi, E. Demler, and M. Knap, arXiv:1504.05956 [Phys. Rev. X (to be published)].
[47] M. Gring, M. Kuhnert, T. Langen, T. Kitagawa, B. Rauer, M. Schreitl, I. Mazets, D. Adu Smith, E. Demler, and J. Schmiedmayer, Science **337**, 1318 (2012).
[48] D. Adu Smith, M. Gring, T. Langen, M. Kuhnert, B. Rauer, R. Geiger, T. Kitagawa, I. Mazets, E. Demler, and J. Schmiedmayer, New J. Phys. **15**, 075011 (2013).
[49] T. Langen, M. Gring, M. Kuhnert, B. Rauer, R. Geiger, D. A. Smith, I. E. Mazets, and J. Schmiedmayer, Eur. Phys. J. Spec. Top. **217**, 43 (2013).
[50] U. Schollwöck, Rev. Mod. Phys. **77**, 259 (2005); Ann. Phys. (Amsterdam) **326**, 96 (2011).
[51] M. Stark and M. Kollar, arXiv:1308.1610.
[52] R. Orbach, Phys. Rev. **112**, 309 (1958).
[53] F. H. L. Essler and R. M. Konik, in *From Fields to Strings: Circumnavigating Theoretical Physics*, edited by M. Shifman, A. Vainshtein, and J. Wheater (World Scientific, Singapore, 2005); arXiv:cond-mat/0412421.
[54] N. Nessi and A. Iucci, arXiv:1503.02507.
[55] A. Iucci and N. Nessi, J. Phys. Conf. Ser. **568**, 012013 (2014).
[56] L. Erdős, M. Salmhofer, and H.-T. Yau, J. Stat. Phys. **116**, 367 (2004).
[57] J. Lukkarinen and H. Spohn, J. Stat. Phys. **134**, 1133 (2009).
[58] See Supplemental Material at http://link.aps.org/supplemental/10.1103/PhysRevLett.115.180601 for more details on the diagonalization of the quadratic part of the Hamiltonian and the derivation of EOM and QBE.

[59] Only states with a fixed particle number are considered in the trace.
[60] In general, the decay times for the real and imaginary parts of the Green's function are different.
[61] B. Bertini, F. H. L. Essler, S. Groha, and N. J. Robinson (to be published).
[62] T. M. Wright, M. Rigol, M. J. Davis, and K. V. Kheruntsyan, Phys. Rev. Lett. **113**, 050601 (2014).
[63] S. Bravyi, M. B. Hastings, and F. Verstraete, Phys. Rev. Lett. **97**, 050401 (2006).
[64] M. L. R. Fürst, C. B. Mendl, and H. Spohn, Phys. Rev. E **86**, 031122 (2012).
[65] J. Lux, J. Müller, A. Mitra, and A. Rosch, Phys. Rev. A **89**, 053608 (2014).
[66] H. Kim, M. C. Banuls, J. I. Cirac, M. B. Hastings, and D. A. Huse, Phys. Rev. E **92**, 012128 (2015).